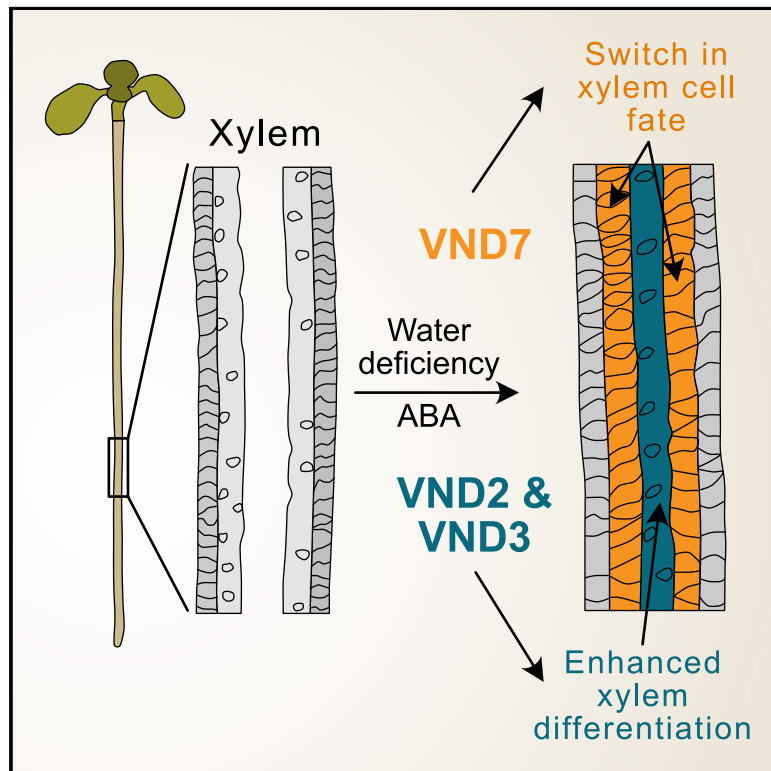


Current Biology

Abscisic acid signaling activates distinct VND transcription factors to promote xylem differentiation in *Arabidopsis*

Graphical abstract



Authors

Prashanth Ramachandran,
Frauke Augstein, Shamik Mazumdar,
Thanh Van Nguyen, Elena A. Minina,
Charles W. Melnyk,
Annelie Carlsbecker

Correspondence

annelie.carlsbecker@ebc.uu.se

In brief

Water limitation triggers ABA signaling to alter xylem development in roots. Ramachandran et al. show that ABA promotes both xylem cell fate change and xylem differentiation rate and that these developmental trajectories are mediated by distinct VND transcription factors. This root xylem response to ABA is conserved among eudicots.

Highlights

- Water limitation promotes cell-autonomous ABA signaling to affect xylem development
- ABA promotes both xylem cell fate change and differentiation rate
- These xylem development effects are mediated by distinct VND transcription factors
- Root xylem developmental ABA response is evolutionarily conserved among eudicots



Report

Abscisic acid signaling activates distinct VND transcription factors to promote xylem differentiation in *Arabidopsis*

Prashanth Ramachandran,^{1,4,5} Frauke Augstein,^{1,5} Shamik Mazumdar,² Thanh Van Nguyen,¹ Elena A. Minina,³ Charles W. Melnyk,² and Annelie Carlsbecker^{1,6,*}

¹Department of Organismal Biology, Physiological Botany, Linnean Centre for Plant Biology, Uppsala University, Ullsv. 24E, SE-756 51 Uppsala, Sweden

²Department of Plant Biology, Linnean Center for Plant Biology, Swedish University of Agricultural Sciences, Ullsv. 24E, SE-756 51 Uppsala, Sweden

³Department of Molecular Sciences, Linnean Center for Plant Biology, Swedish University of Agricultural Sciences, Ullsv. 24E, SE-756 51 Uppsala, Sweden

⁴Present address: Department of Biology, Stanford University, 371 Jane Stanford Way, Stanford, CA 94305, USA

⁵These authors contributed equally

⁶Lead contact

*Correspondence: annelie.carlsbecker@ebc.uu.se

<https://doi.org/10.1016/j.cub.2021.04.057>

SUMMARY

Plants display remarkable abilities to adjust growth and development to environmental conditions, such as the amount of available water. This developmental plasticity is apparent not only in root and shoot growth rates, but also in tissue patterning and cell morphology.^{1,2} We have previously shown that in response to limited water availability, *Arabidopsis thaliana* root displays changes in xylem morphology, mediated by the non-cell-autonomous action of abscisic acid, ABA.² Here, we show, through analyses of ABA response reporters and tissue-specific suppression of ABA signaling, that xylem cells themselves act as primary signaling centers governing both xylem cell fate and xylem differentiation rate, revealing the cell-autonomous control of multiple aspects of xylem development by ABA. ABA rapidly activates the expression of genes encoding VASCULAR-RELATED NAC DOMAIN (VND) transcription factors. Molecular and genetic analyses revealed that the two ABA-mediated xylem developmental changes are regulated by distinct members of this transcription factor family, with VND2 and VND3 promoting differentiation rate of metaxylem cells, while VND7 promotes the conversion of metaxylem toward protoxylem morphology. This phenomenon shows how different aspects of developmental plasticity can be interlinked, yet genetically separable. Moreover, similarities in phenotypic and molecular responses to ABA in diverse species indicate evolutionary conservation of the ABA-xylem development regulatory network among eudicots. Hence, this study gives molecular insights into how environmental stress modifies plant vascular anatomy and has potential relevance for water use optimization and adaptation to drought conditions.

RESULTS AND DISCUSSION

ABA affects both xylem cell fate and differentiation rate

Water-limiting conditions trigger the formation of multiple protoxylem-like cells with spiral secondary cell walls (SCWs) in place of metaxylem with pitted SCWs (Figures 1A–1C, 1E, and S1B).^{2,3} This effect is partly dependent on endodermal abscisic acid (ABA) signaling resulting in enhanced levels of microRNA165 (miR165), which acts non-cell-autonomously to suppress target HOMEODOMAIN-LEUCINE ZIPPER class III (HD-ZIPIII) transcription factors within the stele, thus promoting protoxylem over metaxylem cell fate.^{4,5} However, whether ABA signaling affects other aspects of xylem development and if it could act cell-autonomously is not clear. To further assess ABA's effect on xylem formation, we analyzed if it could affect xylem differentiation

rate by measuring the distance from root tip to point of lignified SCWs detected in wild type (Col-0) after treatment with 1 μ M ABA. Previous analyses have shown this treatment to be a good proxy for water-limiting conditions without negative root growth effects (Figure S1A).² A 48 h ABA treatment caused cells occupying the outer protoxylem (ρx) position of the xylem axis (Figures 1A and 1B) to differentiate slightly closer to the tip (ρx mock, $1,264 \pm 139 \mu\text{m}$ [SD] versus ABA, $1,060 \pm 240 \mu\text{m}$), whereas the neighboring outer metaxylem cells (omx) differentiated significantly closer to the tip (omx mock, $2,950 \pm 374 \mu\text{m}$ versus ABA, $1,912 \pm 393 \mu\text{m}$; Figures 1F and 1G). However, while omx cells normally have pitted SCWs characteristic of metaxylem cells, they frequently formed reticulate or spiral SCW upon ABA treatment, thus becoming protoxylem-like (Figures 1C, 1E, and S1B).² Because protoxylem cells normally



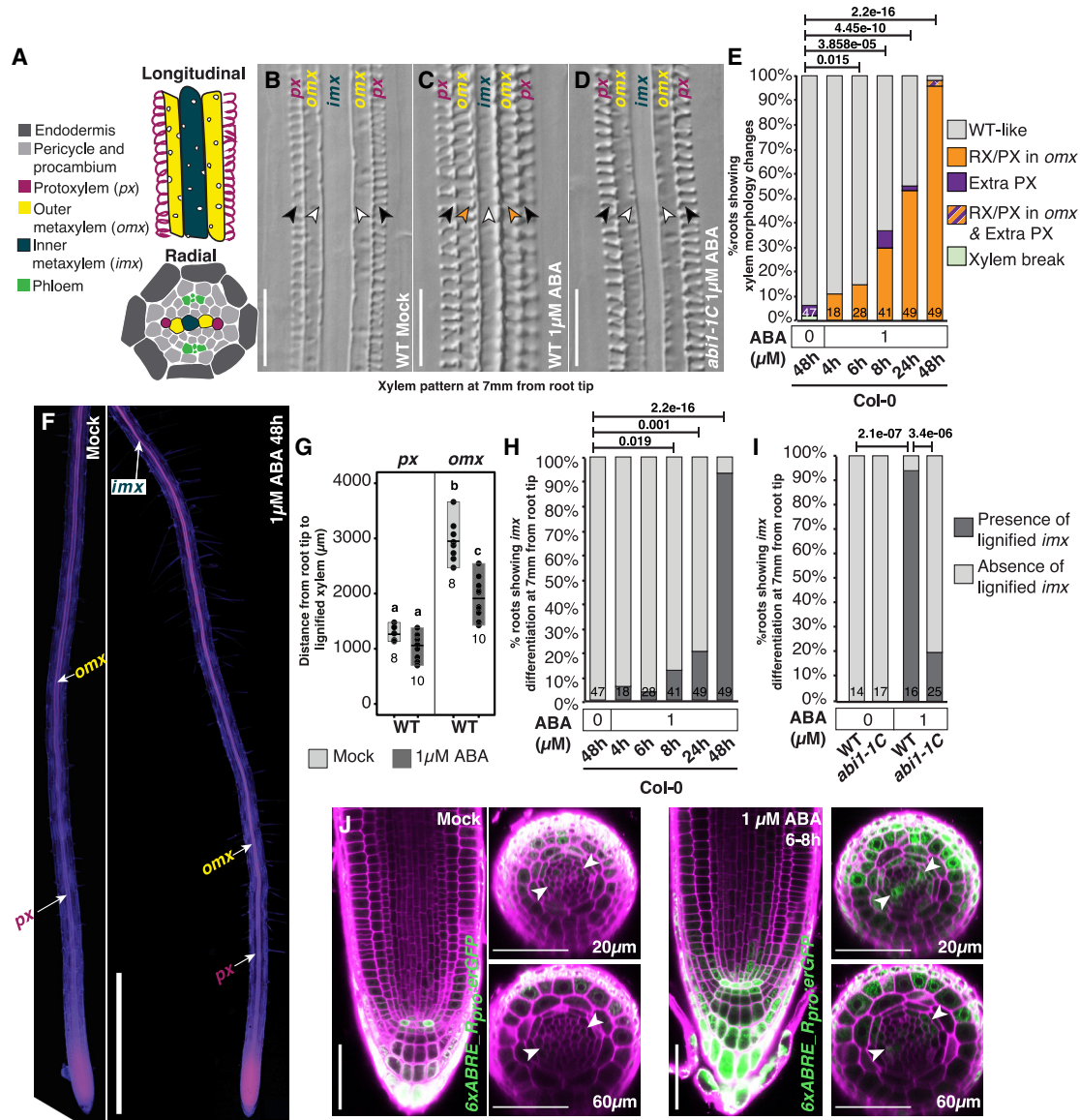


Figure 1. ABA affects both xylem differentiation fate and rate

(A) Cartoon of a longitudinal and cross-section of the *Arabidopsis* root stele (+endodermis in the cross-section) showing different cell types, highlighting the different positions in the xylem axis, *px*, *omx*, and *imx*.

(B–D) Differential interference contrast (DIC) images of the xylem pattern at 7 mm from the root tip after mock and ABA treatment in wild type (WT; B and C) and ABA treatment in *abi1-1C* (D). Differentiated protoxylem vessels are indicated by black arrowheads, metaxylem by white arrowheads, and reticulate xylem by orange arrowheads. *px*, protoxylem position; *omx*, outer metaxylem position; *imx*, inner metaxylem position. Scale bars, 50 μ m.

(E) Temporal analysis of xylem morphology changes in WT roots after 1 μ M ABA treatment for 4, 6, 8, 24, and 48 h. For the 4, 6, and 8 h ABA treatments, the total treatment time before root xylem analysis was 24 h. RX, reticulate xylem; PX, protoxylem.

(F) Mock- and ABA-treated WT roots double stained with basic fuchsin (magenta) and calcofluor white (blue). Pink, yellow, and blue-green text with white arrows indicate the first occurrence of a fuchsin-stained xylem vessel in the *px*, *omx*, and *imx* positions, respectively. Under mock conditions, differentiated xylem in the *imx* position was detected at a distance of 15–20 mm from the root tip (Figure S3H) and is not included within the imaged region of the root. Scale bar, 1 mm.

(G) Quantification of distances from the root tip to lignified vessel in *px* (left) and *omx* (right) positions. In the *px* position, vessels had spiral SCWs under both mock and ABA treatments, while *omx* vessels had pitted SCWs under mock and pitted, reticulate, or spiral SCWs under ABA treatment. Difference in morphology of *omx* vessels was not considered for the quantification of distances. Black filled dots represent measurements from individual roots.

(H) Quantification of early *imx* differentiation; graph shows presence/absence of lignified *imx* xylem vessel at 7 mm from the root tip, after 1 μ M ABA treatment. Treatment times are as in (E).

(I) Frequency of early *imx* differentiation as in (H) in WT and *abi1-1C* after 48 h 1 μ M ABA treatment.

(legend continued on next page)

differentiate closer to the root tip, the earlier *omx* differentiation observed may be coupled to cell fate changes. In contrast, the inner metaxylem cells (*imx*) (Figure 1A) never formed reticulate or spiral SCWs upon 1 μ M ABA treatment (Figure 1C). In 5-day-old mock-treated seedlings, *imx* differentiated 15–20 mm from the root tip, with 0% showing differentiated *imx* at 7 mm from the root tip (Figure S3H). After 48 h 1 μ M ABA treatment, 94% displayed differentiated *imx* at 7 mm from the root tip (Figure 1H), suggesting that ABA promotes metaxylem differentiation rate independent of its effect on xylem morphology. Transverse sections showed that ABA's effect was restricted to the xylem cells (Figure S1C). Furthermore, transferring back to mock conditions restored both xylem morphology and differentiation rate within 48 h (Figures S1D–S1F), further corroborating that xylem formation is highly plastic.

The dominant *ABA-INSENSITIVE1* mutant (*abi1-1*), in which ABA signaling is suppressed even in the presence of ABA,^{6,7} strongly reduced the effects of ABA treatment on early *imx* differentiation (20% in *abi1-1* versus 94% in wild type; Figures 1D, 1I, and S1C), and on xylem fate change in *omx* (Figure S1G),² showing that canonical ABA signaling is important for xylem differentiation. However, while endodermal ABA signaling repression (using *SCR_{pro}:abi1-1*) significantly suppressed *omx* fate change (Figure S1H),² it had less effect on the enhanced differentiation (65% versus 100%; Figure S1I), suggesting that signaling in other cell types contributed to this response. To determine where ABA response occurs, we used synthetic ABA responsive reporters with tandem ABA RESPONSIVE ELEMENT (ABRE) repeats from two ABA responsive genes, *ABI1* and *RAB18* (*6XABRE_{pro}:GFP_{er}* and *6XABRE_{pro}:GFP_{er}*), respectively, which were previously described.⁸ While both reporters showed strong QC and lateral root cap expression under mock conditions, optical cross-sections revealed weak expression in epidermis, cortex, endodermis, pericycle, and protoxylem precursor cells, suggesting that ABA signaling occurs in these tissues under non-stressed conditions (Figures 1J and S1J). After 6–8 h treatment with 1 μ M ABA, signal intensity of both reporters increased in these tissues, and within the stele the xylem precursor cells displayed an ABA response maximum (Figures 1J and S1K). Next, we simulated water deficiency by growing plants on polyethylene glycol (PEG) overlaid media² (Figure S1L). This resulted in similar but stronger ABA response suggesting that exogenous ABA treatment could recapitulate cell-specific ABA responses occurring during water deprivation.

ABA signaling within the xylem activates VND transcription factors

The ABA response profile prompted us to investigate the importance of ABA signaling in different tissues for xylem differentiation. We analyzed F1 progeny of *UAS_{pro}:abi1-1*⁹ crossed with enhancer trap lines J1721, expressing in the xylem axis, QC, and columella; Q0990, procambium; or J0571, ground tissue,

upon ABA treatment (Figures 2A and S2A). Similar to its effect on wild type, root growth of the transactivation lines was not negatively affected by ABA treatment (Figure S2D). Strikingly, the *J1721>>abi1-1* line efficiently suppressed ABA's effects on both xylem differentiation rate and fate (Figures 2B, 2C, and S2B). Neither *Q0990>>abi1-1* nor *J0571>>abi1-1* could suppress xylem differentiation rate, but consistent with our previous observations,² *J0571>>abi1-1* partially suppressed xylem fate changes (Figures 2B, 2C, and S2B). Furthermore, while mock-treated *J0571>>abi1-1* occasionally displayed discontinuous metaxylem,² this was not detected in either of the stele-active lines (Figures S2B and S2C). These results suggest that ABA signaling in the stele is not critical for xylem formation per se, but that signaling within the xylem cells is essential to determine both xylem differentiation rate and xylem cell fate upon conditions causing elevated ABA levels.

To identify the genetic regulators involved in stress-mediated xylem developmental changes, we performed RNA sequencing (RNA-seq) of 8 h ABA-treated Col-0 roots and identified 2,368 genes upregulated by ABA (\log_2 FC > 0.5; $p_{\text{adj}} < 0.05$; Figure 2D; Data S1A). Of these, 114 were identified as xylem expressed by comparing with xylem-enriched genes from a single-cell RNA-seq study¹⁰ (Figure 2D; Data S1A). ABA-responding xylem genes included *CELLULOSE SYNTHASE4* (*CESA4*), *CESA7*, *CESA8*, *LACCASE11* (*LAC11*), *LAC17*, *XYLEM CYSTEINE PEPTIDASE1* (*XCP1*), and *XCP2*, as well as genes encoding transcription factors *MYB46*, *MYB83*, *VND2*, *VND3*, and *VND7* that act upstream of many SCW biosynthesis genes^{11–15} (Data S1A; Figure 3F). In line with ABA signaling acting within the xylem cells, RNA-seq of ABA-treated *J1721>>abi1-1* revealed a reduced activation of a subset of these genes, including the *CESAs*, *LAC17*, *MYB46*, *MYB83*, and *VND3* (Figure 2D; Data S1C; $p < 0.05$).

Independent qRT-PCR analyses on ABA-treated wild-type root tips were consistent with the RNA-seq (Figure 2F), and additionally showed that 2 h treatment was sufficient to significantly upregulate not only *VND1*, *VND2*, *VND3*, and *VND7*, but also *VND4*. Longer treatment times induced *VND5*, whereas *VND6*, a regulator of metaxylem differentiation,¹² was not upregulated. A direct influence of ABA specifically on *VND1*, 2, 3, and 7 is supported by promoter binding of ABRE BINDING FACTORS (ABFs) and other ABA-related transcription factors¹⁶ (Table S1). Furthermore, independent qRT-PCR testing of ABA's effect on *abi1-1* transactivation lines showed a significant suppression of *VND2* activation by *J1721>>abi1-1* with *VND3* displaying a similar trend (Figures 2E and S2E). Transcriptional reporter lines¹² revealed distinct expression patterns for *VND1*, *VND2*, and *VND3* in immature xylem cells within the meristem, with *VND1* restricted to *omx* cells, *VND2* to all metaxylem precursor cells (*omx* and *imx*), while *VND3* expression was observed in *px*, *omx*, and *imx* cells (Figure 2G). *VND3* expression extended into the differentiation zone, while *VND1* and *VND2* were restricted to the meristem (Figures 2G and S2F). *VND7*

(J) Confocal micrographs of the ABA response domains in the root apical meristem visualized using *6xABRE_{pro}:erGFP* after mock or 1 μ M ABA treatment. Radial optical sections were captured at 20 μ m and 60 μ m shootward of the quiescent center (QC). Magenta, propidium iodide; green, GFP. White arrowheads indicate the xylem axis. Scale bars, 50 μ m.

Statistics in (E), (H), and (I): values above the bar represent p values from Fisher's exact test, incorporating all phenotype categories. In (G), a,b,c represent groups with significant differences, one-way ANOVA with Tukey's post hoc testing ($p < 0.05$). Numbers at the bottom of the bars in (E) and (G)–(I) represent number of roots analyzed. See also Figure S1 and Data S2.

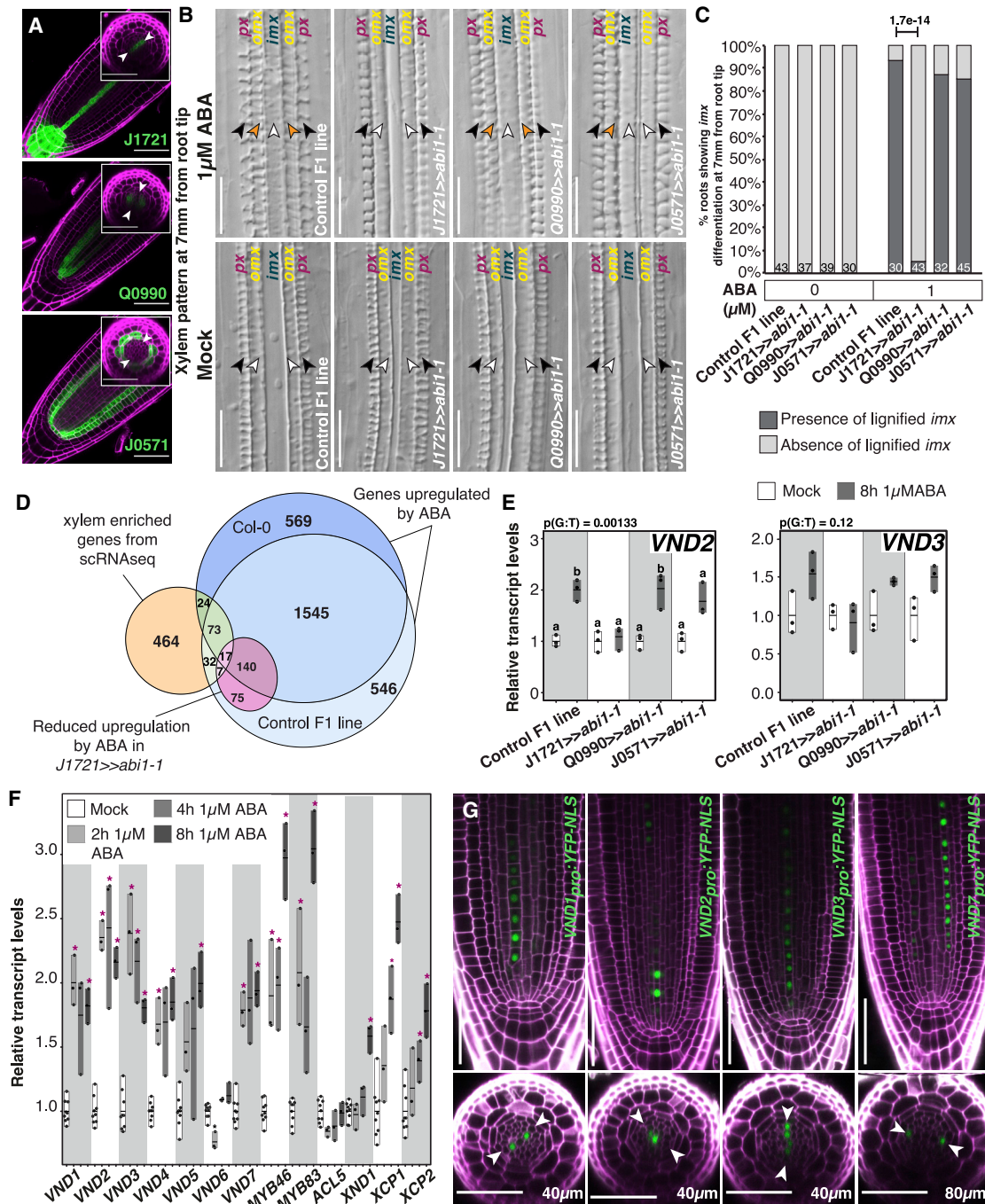


Figure 2. ABA signaling within the xylem activates VND transcription factors

(A) Confocal micrographs representing the activity domains of the J0571, Q0990, and J1721 GAL4 enhancer trap lines (green) imaged in F1 plants resulting from crosses with *UAS_{pro}:abi1-1*. Insets show radial optical sections of each enhancer trap line; arrowheads mark the xylem axis.

(B) DIC images of the xylem pattern in 48 h 1 μ M ABA- and mock-treated *abi1-1* transactivation lines. Control F1 is *UAS_{pro}:abi1-1* (Col-0) X C24. Differentiated protoxylem vessels are indicated by black arrowheads, metaxylem by white arrowheads, and reticulate xylem by orange arrowheads. *px*, protoxylem position, *omx*, outer metaxylem position; *imx*, inner metaxylem position.

(C) Quantification of early *imx* differentiation after mock and 1 μ M ABA treatment in different *abi1-1* transactivation lines, as measured by presence/absence of lignified xylem at 7 mm from the root tip. Values above the bar represent p values from Fisher's exact test incorporating all phenotype categories. Numbers at the bottom of the bars indicate number of roots analyzed.

(D) Venn diagram showing the overlap of genes upregulated by ABA in Col-0 and in control F1 with genes enriched in xylem expression according to single-cell RNA-seq.¹⁰ A subset of these genes (pink) showed reduced upregulation in lines where ABA signaling was suppressed by *J1721>>abi1-1*, $p < 0.05$.

(E) Relative transcript levels of *VND2* and *VND3* in Control F1 line, *J1721>>abi1-1*, *Q0990>>abi1-1*, and *J0571>>abi1-1* lines under Mock and 8h 1 μ M ABA treatment. p(G:T) = 0.00133 for *VND2* and p(G:T) = 0.12 for *VND3*.

(F) Relative transcript levels of *VND1*, *VND2*, *VND3*, *VND4*, *VND5*, *VND6*, *VND7*, *MYB46*, *MYB63*, *ACL5*, *XND1*, *XCP1*, and *XCP2* in Control F1 line, *J1721>>abi1-1*, *Q0990>>abi1-1*, and *J0571>>abi1-1* lines under Mock, 2h 1 μ M ABA, 4h 1 μ M ABA, and 8h 1 μ M ABA treatments. Asterisks indicate significant differences.

(G) DIC images of *VND1_{pro}:YFP-NLS*, *VND2_{pro}:YFP-NLS*, *VND3_{pro}:YFP-NLS*, and *VND5_{pro}:YFP-NLS* activity in Control F1 line, *J1721>>abi1-1*, *Q0990>>abi1-1*, and *J0571>>abi1-1* lines under Mock and 8h 1 μ M ABA treatments. Arrowheads mark the xylem axis.

(legend continued on next page)

expressed specifically in protoxylem precursors within the meristem, but extended into differentiating protoxylem cells (Figures 2G and S2J),¹¹ while *VND5* was only detected in differentiating protoxylem strands with the close paralog *VND4* displaying a similar pattern (Figure S2F).¹² Thus, only *VND1*, *VND2*, *VND3*, and *VND7* act in early xylem development and potentially directly downstream of ABA signaling. We, therefore, focused primarily on these factors, and analyzed the effect of 6–8 h 1 μ M ABA treatment on the reporters for these genes. While expression levels increased, none of the reporters displayed obvious expression pattern changes (Figures S2G–S2J). However, after treatment with higher concentration of ABA, *VND7* has been reported to expand into the *omx* cell lineage within the meristem.³ Taken together, these data show that *VND* expression levels rapidly and specifically increase within the xylem precursor cells upon increased ABA levels.

VNDs regulate plasticity in xylem fate and xylem differentiation rate

To test if VND transcription factors are required for the ABA-induced xylem developmental changes, we analyzed *vnd* mutants after ABA treatment and growth under water-limiting conditions. Single and most double mutants of *vnd1*, *vnd2*, *vnd3*, and *vnd7* displayed wild-type-like xylem patterns (Figure S3A). However, *vnd2vnd3* (*vnd2,3*) and *vnd1vnd2vnd3* (*vnd1,2,3*) had discontinuous metaxylem strands (Figures 3A and 3B), and in *vnd1,2,3*, metaxylem strands in *omx* and *imx* positions frequently failed to differentiate (Figures 3B and 3D). Upon ABA treatment, *vnd2,3* and *vnd1,2,3* did not show the early *imx* differentiation that occurs in wild-type plants (Figures 3A, 3C, S3B, S3C, and S3H). Importantly, the same effect was detected upon growth on water-limiting conditions, although root growth inhibition occurred in these mutants similarly to wild type (Figures 3D, 3E, S3E, and S3F). Hence, *VND2* and *VND3* are required to promote early *imx* differentiation upon enhanced ABA signaling and under water-limiting conditions.

Despite a role in *imx* differentiation rate, *vnd2,3* and *vnd1,2,3* displayed early *omx* differentiation and protoxylem-like or reticulate *omx* morphology upon ABA treatment (Figures 3A, 3B, and S3G). In contrast, the cell fate change was suppressed in *vnd7* (Figures 3A and 3B), while it displayed early *omx* and *imx* differentiation (Figures 3C, S3G, and S3H). Hence, ABA treatment of *vnd7* revealed a previously uncharacterized requirement for *VND7* in xylem cell fate change from metaxylem toward protoxylem-like cells. Furthermore, these data show that ABA's effect on xylem differentiation rate and xylem cell fate change can be genetically separated via the activation of distinct VND genes.

To further dissect how the VNDs regulate xylem developmental plasticity, we analyzed the transcriptomic effects of

ABA treatment in *vnd1,2,3* and *vnd7* (Data S1A; Figure S3I). Under mock conditions, 53 xylem-enriched genes were significantly reduced in the *vnd1,2,3* mutant ($\log_2FC < 0.5$; $p_{adj} < 0.05$; Data S1B). Consistent with the wild-type-like phenotype of *vnd7*, only three xylem-enriched genes were significantly reduced in this background. Under ABA induction, *vnd1,2,3* could significantly reduce the upregulation of 21 xylem-expressed genes including the two *XCP* genes, *CESA4*, *LAC11*, and *17*, but not *MYB46* and *MYB83* (Data S1A), suggesting that these factors are regulated by ABA independently of *VND1*, *2*, and *3*. This finding is further supported by ABF binding to the promoter of *MYB46* (Table S1).¹⁶ *vnd7* had little effect on genes induced by ABA, with only *LAC11* significantly reduced among the xylem-expressed genes (Data S1A). Taken together, these data suggest that while *VND1*, *2*, and *3* are required for normal expression of many xylem differentiation genes, additional factors act redundantly with the VNDs to further promote xylem gene expression upon rising ABA levels.

As *vnd7* could suppress *omx* cell fate change but did not affect differentiation rate upon ABA, we reasoned that *VND7* might act redundantly with *VND1*, *2*, and *3* to regulate this trait, and we therefore generated the *vnd1vnd2vnd3vnd7* mutant. Here, both the ABA-induced *omx* fate change and the premature *imx* differentiation were suppressed (Figures 3G and S3J), showing the additivity of the two phenotypes assigned to *vnd7* and *vnd123*, respectively. However, although *omx* cells maintained metaxylem morphology, they could still respond to ABA with faster differentiation, similar to wild type (Figures 3G and 3H). Hence, factors other than *VND1*, *VND2*, *VND3*, and *VND7* govern the early *omx* differentiation induced by high ABA levels. Our transcriptome datasets indicate that *MYB46* and *MYB83* are potential candidates for this role.

ABA promotes xylem differentiation in several eudicot species

Overexpression of VND transcription factors induced the formation of ectopic xylem tracheary element cells.^{12,15} Since ABA had a positive effect on the expression of a number of xylem differentiation genes including the VNDs, we tested ABA's capacity to induce trans-differentiation of cotyledon mesophyll into xylem cells, as previously seen upon treatment with auxin and cytokinin along with bikinin (an inhibitor of GSK3 kinases involved in brassinosteroid signaling).¹⁷ Strikingly, substitution of bikinin for ABA resulted in ectopic lignification, although cells did not form a typical xylem SCW pattern (Figures 4A and 4B). The ectopic lignification was nonetheless suppressed both in *abi1-1* and in *vnd1,2,3* and *vnd7* mutants (Figures S4A–S4C), suggesting that the ectopic lignification is a specific effect of the ABA treatment and that *VND1*, *2*, *3*, and *7* regulate this effect.

(E) Relative transcript levels of *VND2* and *VND3* after 8 h ABA treatment in whole roots of F1 seedlings from crosses between *UAS_{pro}:abi1-1* and indicated GAL4 enhancer trap lines, using qRT-PCR. The significance of genotype:treatment (G:T) interaction on gene expression based on a two-way ANOVA analysis is given above the plots. Letters *a* and *b* represent groups with significant differences with Tukey's post hoc testing ($p < 0.05$).

(F) qRT-PCR quantification of xylem developmental gene transcript levels in 1 mm WT root tips after 2, 4, and 8 h of 1 μ M ABA treatment. * $p < 0.05$, two-tailed Student's *t* test.

In (E) and (F), all values are normalized to the average of respective mock-treated samples.

(G) Confocal images of *VND1*, *VND2*, *VND3*, and *VND7* promoter activity domains in root meristem longitudinal and radial planes. Distances from QC where the radial images were captured are indicated in the images. White arrowheads indicate xylem axis.

Scale bars in (A), (B), and (G), 50 μ m. See also Figure S2 and Data S1 and S2.

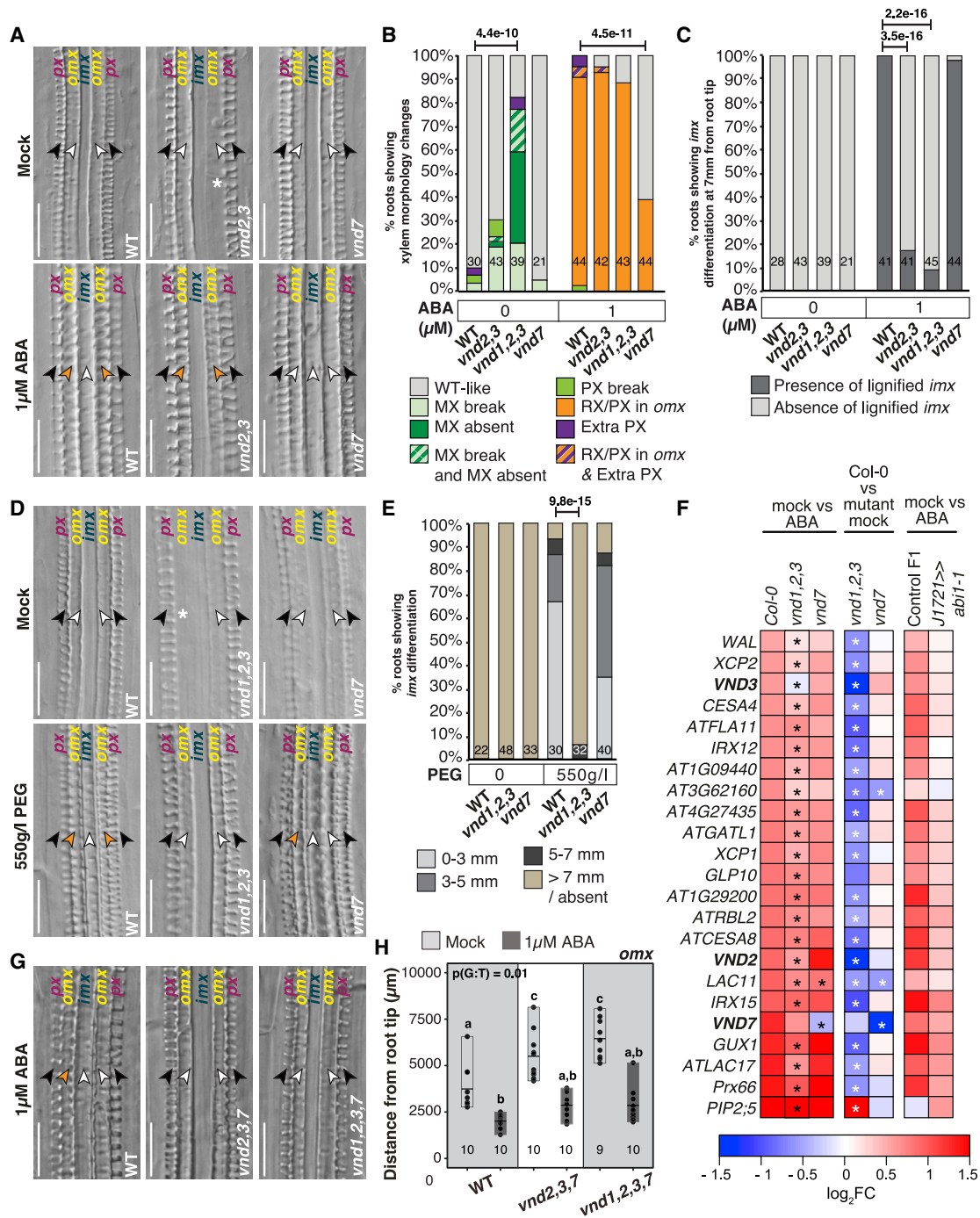


Figure 3. VNDs regulate plasticity of xylem fate and differentiation rate

(A) Representative DIC images of mock- and ABA-treated wild type (WT), *vnd2 vnd3* (*vnd2,3*), and *vnd7* roots at 7 mm from the root tip. In (A), (D), and (G), px, protoxylem position; omx, outer metaxylem position; imx, inner metaxylem position. Differentiated protoxylem vessels are indicated by black arrowheads, metaxylem by white arrowheads, and reticulate xylem by orange arrowheads. Asterisk (*) indicates xylem break. Scale bars, 50 μ m.

(B and C) Quantification of xylem morphology (B) and *imx* differentiation at 7 mm from the root tip (C) in *vnd2,3*, *vnd1 vnd2 vnd3* (*vnd1,2,3*), and *vnd7*.

(D) Representative DIC images of mock- and polyethylene glycol (PEG)-treated WT, *vnd1,2,3*, and *vnd7* roots.

(E) Quantification of distances at which differentiated *imx* was detected in WT, *vnd1,2,3*, and *vnd7* roots subjected to mock or PEG treatments.

(F) Heatmap of xylem-enriched genes upregulated by ABA in WT ($\log_2FC > 0.5$, $p_{adj} < 0.05$) and with a reduced activation by ABA in *vnd1,2,3* or *vnd7* and their pattern in *J1721>>abi1-1* lines. Black asterisks indicate significantly reduced activation upon ABA in mutants compared to WT ($p_{adj} < 0.05$); white asterisks indicate downregulation in mutants compared to WT under mock conditions.

(legend continued on next page)

To examine if xylem responses upon stress are a conserved trait, we analyzed root xylem upon ABA treatment in five different eudicot species (Figures 4C–4E and S4D–S4F). This revealed that *Brassica napus* and *Brassica rapa* (Brassicales, Rosidae), *Nicotiana benthamiana* and *Solanum lycopersicum* (Solanales, Asteridae), and *Phtheirospermum japonicum* (Lamiales, Asteridae) all displayed early xylem differentiation and a higher number of xylem strands compared to mock condition, similar to *Arabidopsis* (Figures 4C–4E and S4D–S4F). Consistent with our observation, an effect of ABA on root xylem development in tomato was previously found.³ We observed a 10-fold upregulation of the putative tomato *VND1*, *VND2*, and *VND3* ortholog (*Solyco02 g083450*) and a 4-fold upregulation of the *VND4-VND5* ortholog (*Solyco08 g079120*) after 6 h of 1 μ M ABA treatment (Figure 4F). The ABA treatment had a small positive effect on one of the two *VND6* orthologs and no significant effect on tomato's two *VND7* orthologs. These results suggest at least a partial conservation in molecular and phenotypic responses to ABA among eudicots.

Taken together, here we provide insights into the molecular regulation underlying xylem developmental plasticity in *Arabidopsis*. We show that ABA signaling in the xylem precursors triggers alterations in xylem cell developmental trajectories, affecting both fate and rate of differentiation, through the activation of distinct xylem-expressed transcriptional regulators belonging to the VND gene family (Figure 4G). However, ABA also acts non-cell-autonomously via miR165 activation in the endodermis, reducing levels of HD-ZIPIII transcription factors in the stele (Figure 4G).^{2,3} Intriguingly, both pathways appear important for xylem cell fate determination. While gene regulatory network studies have uncovered a complex interplay between VND and HD-ZIPIII transcription factors,¹⁸ it remains unclear how these factors temporally interact within the pluripotent xylem precursor cells to determine xylem cell fate, under normal growth conditions and during stress.

The two distinct phenotypic changes observed under ABA treatment and water-limiting conditions may contribute two distinct advantages to the plant. A change toward more protoxylem-like cells may reduce risk of detrimental effects of air bubbles, embolisms, interrupting water transport. This is because protoxylem strands are thinner, but also may enhance lateral water movement between xylem strands for embolism repair.¹⁹ Early metaxylem formation resulting in increased xylem area, on the other hand, may enhance hydraulic conductance and increase drought resistance.²⁰ Furthermore, a recent study described a maize mutant defective in a VND homolog that displayed symptoms of water stress under normal conditions due to defective protoxylem cells in adult plants.²¹ This suggests that VND-dependent xylem cell acclimation to stress is a trait that evolved prior to the divergence of monocots and eudicots. Thus, ABA-VND regulation may be a potentially universal molecular toolkit for

xylem cell developmental adjustments with utility for breeding of drought-resilient crop plants.

STAR★METHODS

Detailed methods are provided in the online version of this paper and include the following:

- KEY RESOURCES TABLE
- RESOURCE AVAILABILITY
 - Lead contact
 - Materials Availability
 - Data and code availability
- EXPERIMENTAL MODEL AND SUBJECT DETAILS
- METHOD DETAILS
 - Plant growth conditions
 - Phenotypic analysis
 - Confocal analysis
 - Expression analysis by quantitative RT-PCR
 - RNAseq analysis
- QUANTIFICATION AND STATISTICAL ANALYSIS

SUPPLEMENTAL INFORMATION

Supplemental information can be found online at <https://doi.org/10.1016/j.cub.2021.04.057>.

ACKNOWLEDGMENTS

We thank J.R. Dinneny, Stanford University; T. Demura, NAIST; and Nottingham *Arabidopsis* Stock Centre for materials; C. Musseau for tomato VND identifications; and M. Englund for technical assistance. We acknowledge support from the Nilsson Ehle Foundation, Lars Hiertas Minne, Lundell PO scholarship (P.R.), a Wallenberg Academy Fellowship (KAW2016.0274, C.W.M.), Vetenskapsrådet (2017-05122, C.W.M. and S.M.), and Formas (2017-00857, A.C.).

AUTHOR CONTRIBUTIONS

Conceptualization, P.R., A.C., and F.A.; Investigation, P.R., F.A., S.M., and T.V.N.; Writing – Original Draft, P.R.; Writing – Review & Editing, P.R., A.C., C.W.M., and F.A.; Funding Acquisition, P.R., A.C., and C.W.M.; Supervision, A.C., E.A.M., and C.W.M.

DECLARATION OF INTERESTS

The authors declare no competing interests.

Received: October 5, 2020

Revised: February 3, 2021

Accepted: April 22, 2021

Published: May 26, 2021

REFERENCES

1. Finkelstein, R. (2013). Abscisic acid synthesis and response. *Arabidopsis Book 11*, e0166.

(G) DIC images showing xylem pattern in WT, *vnd2,3,7*, and *vnd1 vnd2 vnd3 vnd7 (vnd1,2,3,7)* after 1 μ M ABA treatment.

(H) Quantification of distances from the root tip to *omx* for WT, *vnd2 vnd3 vnd7 (vnd2,3,7)*, and *vnd1,2,3,7*.

Statistics: in (B), (C), and (E), values above the bar represent p values from Fisher's exact test, incorporating all phenotype categories; in (H), the significance of genotype:treatment (G:T) interaction on gene expression based on two-way ANOVA analysis is given in the plot. *a,b,c* represent groups with significant differences with Tukey's post hoc testing ($p < 0.05$). Numbers at the bottom of the bars in (B), (C), (E), and (H) represent the number of roots analyzed. See also Figure S3 and Data S1 and S2.

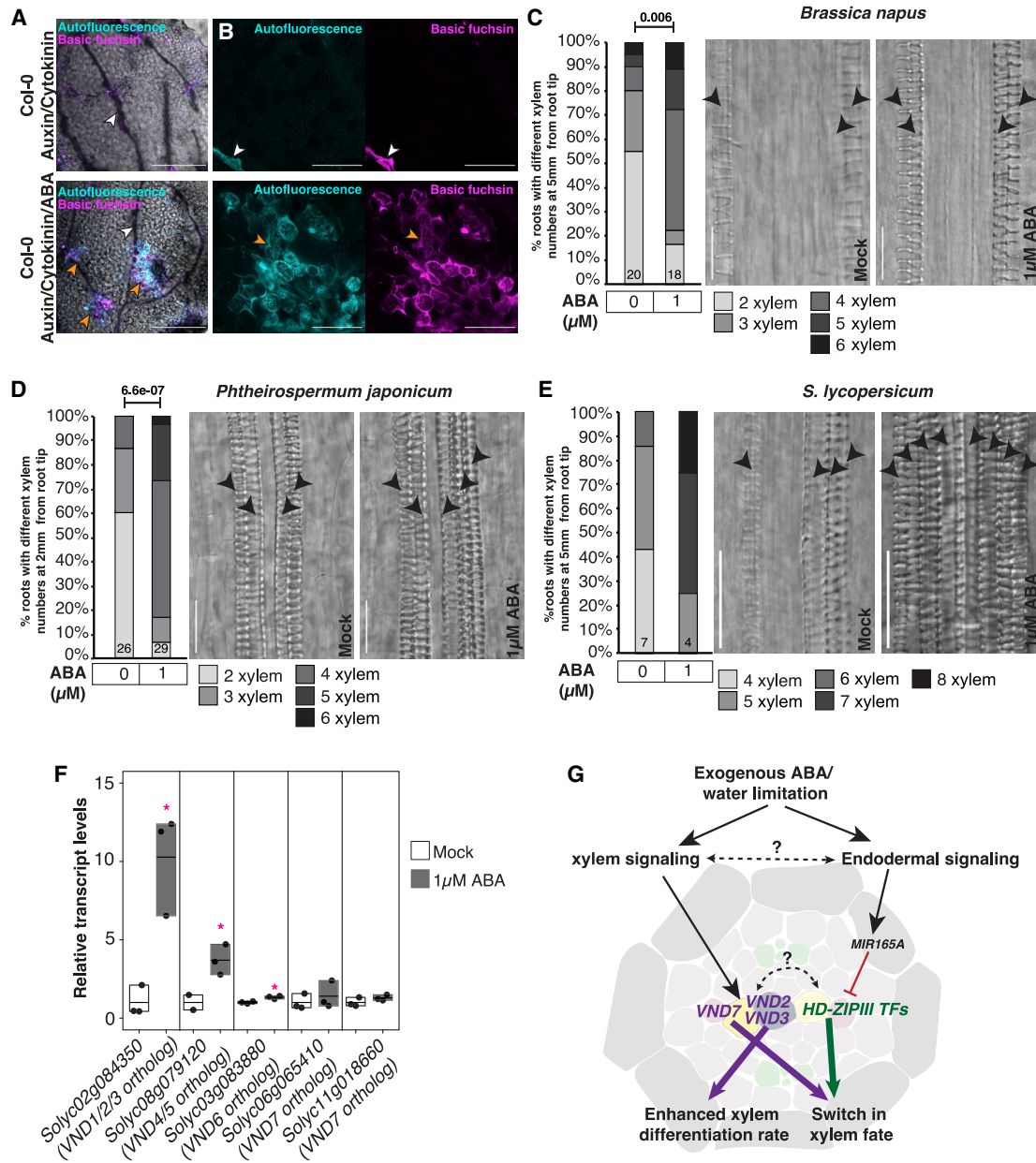


Figure 4. ABA induces ectopic lignification in *Arabidopsis* cotyledons and promotes xylem differentiation in several eudicot species

(A and B) Confocal micrographs showing the formation of ectopic lignification in wild-type (WT) *in vitro* culture in auxin-cytokinin-containing media with or without ABA. Ectopic lignification is visualized using lignin autofluorescence and basic fuchsin staining. Images in (B) show zoomed-in regions of ectopic lignification. White arrowheads indicate cotyledon venation and orange arrowheads indicate ectopic lignin deposition. Scale bars, 500 μm (A) and 100 μm (B). (C–E) Quantification of total number of lignified xylem vessels at specific distances from the root tip in *Brassica napus* (C), *Phtheirospermum japonicum* (D), and *Solanum lycopersicum* (cv. Money Maker) (E) after mock and 1 μM ABA treatment accompanied by representative images. Black arrowheads indicate xylem strands. * $p < 0.05$ (C and D), Fisher's exact test incorporating all phenotype categories. Numbers at the bottom of the bars represent the number of individuals analyzed. Scale bars, 50 μm .

(F) qRT-PCR of *VND* homologs in tomato roots after 1 μM ABA treatment for 6 h. * $p < 0.05$, two-tailed Student's *t* test.

(G) Model showing genetic components regulated by ABA to mediate two different phenotypic effects. ABA signaling in the stele activates *VND2*, *VND3*, and *VND7*. While *VND2* and *VND3* are mainly involved in ABA-mediated enhancement of xylem differentiation rate, *VND7* mediates the switch in xylem morphology from pitted to a spiral or reticulate form. In the endodermis, ABA signaling activates miR165, which moves to downregulate stele-expressed HD-ZIPIII transcription factors resulting in altered xylem fate.^{2,3}

See also Figure S4.

2. Ramachandran, P., Wang, G., Augstein, F., de Vries, J., and Carlsbecker, A. (2018). Continuous root xylem formation and vascular acclimation to water deficit involves endodermal ABA signalling via miR165. *Development* **145**, dev159202.
3. Bloch, D., Pulli, M.R., Mosquna, A., and Yalovsky, S. (2019). Abiotic stress modulates root patterning via ABA-regulated microRNA expression in the endodermis initials. *Development* **146**, dev177097, dev29.
4. Carlsbecker, A., Lee, J.-Y., Roberts, C.J., Dettmer, J., Lehesranta, S., Zhou, J., Lindgren, O., Moreno-Risueno, M.A., Vatén, A., Thitamadee, S., et al. (2010). Cell signalling by microRNA165/6 directs gene dose-dependent root cell fate. *Nature* **465**, 316–321.
5. Miyashima, S., Koi, S., Hashimoto, T., and Nakajima, K. (2011). Non-cell-autonomous microRNA165 acts in a dose-dependent manner to regulate multiple differentiation status in the Arabidopsis root. *Development* **138**, 2303–2313.
6. Leung, J., Bouvier-Durand, M., Morris, P.C., Guerrier, D., Chedford, F., and Giraudat, J. (1994). Arabidopsis ABA response gene ABI1: features of a calcium-modulated protein phosphatase. *Science* **264**, 1448–1452.
7. Meyer, K., Leube, M.P., and Grill, E. (1994). A protein phosphatase 2C involved in ABA signal transduction in Arabidopsis thaliana. *Science* **264**, 1452–1455.
8. Wu, R., Duan, L., Pruneda-Paz, J.L., Oh, D.-H., Pound, M., Kay, S., and Dinneny, J.R. (2018). The 6xABRE synthetic promoter enables the spatio-temporal analysis of ABA-mediated transcriptional regulation. *Plant Physiol.* **177**, 1650–1665.
9. Duan, L., Dietrich, D., Ng, C.H., Chan, P.M.Y., Bhalerao, R., Bennett, M.J., and Dinneny, J.R. (2013). Endodermal ABA signaling promotes lateral root quiescence during salt stress in Arabidopsis seedlings. *Plant Cell* **25**, 324–341.
10. Denyer, T., Ma, X., Klesen, S., Scacchi, E., Nieselt, K., and Timmermans, M.C.P. (2019). Spatiotemporal developmental trajectories in the Arabidopsis root revealed using high-throughput single-cell RNA sequencing. *Dev. Cell* **48**, 840–852.e5.
11. Zhong, R., and Ye, Z.-H. (2012). MYB46 and MYB83 bind to the SMRE sites and directly activate a suite of transcription factors and secondary wall biosynthetic genes. *Plant Cell Physiol.* **53**, 368–380.
12. Kubo, M., Udagawa, M., Nishikubo, N., Horiguchi, G., Yamaguchi, M., Ito, J., Mimura, T., Fukuda, H., and Demura, T. (2005). Transcription switches for protoxylem and metaxylem vessel formation. *Genes Dev.* **19**, 1855–1860.
13. Endo, H., Yamaguchi, M., Tamura, T., Nakano, Y., Nishikubo, N., Yoneda, A., Kato, K., Kubo, M., Kajita, S., Katayama, Y., et al. (2015). Multiple classes of transcription factors regulate the expression of VASCULAR-RELATED NAC-DOMAIN7, a master switch of xylem vessel differentiation. *Plant Cell Physiol.* **56**, 242–254.
14. Yamaguchi, M., Mitsuda, N., Ohtani, M., Ohme-Takagi, M., Kato, K., and Demura, T. (2011). VASCULAR-RELATED NAC-DOMAIN7 directly regulates the expression of a broad range of genes for xylem vessel formation. *Plant J.* **66**, 579–590.
15. Zhou, J., Zhong, R., and Ye, Z.-H. (2014). Arabidopsis NAC domain proteins, VND1 to VND5, are transcriptional regulators of secondary wall biosynthesis in vessels. *PLoS ONE* **9**, e105726.
16. Song, L., Huang, S.C., Wise, A., Castanon, R., Nery, J.R., Chen, H., Watanabe, M., Thomas, J., Bar-Joseph, Z., and Ecker, J.R. (2016). A transcription factor hierarchy defines an environmental stress response network. *Science* **354**, aag1550.
17. Kondo, Y., Fujita, T., Sugiyama, M., and Fukuda, H. (2015). A novel system for xylem cell differentiation in Arabidopsis thaliana. *Mol. Plant* **8**, 612–621.
18. Taylor-Teeples, M., Lin, L., de Lucas, M., Turco, G., Toal, T.W., Gaudinier, A., Young, N.F., Trabucco, G.M., Veling, M.T., Lamothe, R., et al. (2015). An Arabidopsis gene regulatory network for secondary cell wall synthesis. *Nature* **517**, 571–575.
19. Hwang, B.G., Ryu, J., and Lee, S.J. (2016). Vulnerability of protoxylem and metaxylem vessels to embolisms and radial refilling in a vascular bundle of maize leaves. *Front. Plant Sci.* **7**, 941.
20. Tang, N., Shahzad, Z., Lonjon, F., Loudet, O., Vaillau, F., and Maurel, C. (2018). Natural variation at XND1 impacts root hydraulics and trade-off for stress responses in Arabidopsis. *Nat. Commun.* **9**, 3884.
21. Dong, Z., Xu, Z., Xu, L., Galli, M., Gallavotti, A., Dooner, H.K., and Chuck, G. (2020). *Necrotic upper tips1* mimics heat and drought stress and encodes a protoxylem-specific transcription factor in maize. *Proc. Natl. Acad. Sci. USA* **117**, 20908–20919.
22. Regner, F., da Câmara Machado, A., da Câmara Machado, M.L., Steinkellner, H., Mattanovich, D., Hanzer, V., Weiss, H., and Katinger, H. (1992). Coat protein mediated resistance to plum pox virus in *Nicotiana glauca* and *N. benthamiana*. *Plant Cell Rep.* **11**, 30–33.
23. Ishida, J.K., Yoshida, S., Ito, M., Namba, S., and Shirasu, K. (2011). Agrobacterium rhizogenes-mediated transformation of the parasitic plant *Phtheirospermum japonicum*. *PLoS ONE* **6**, e25802.
24. Verslues, P.E., and Bray, E.A. (2006). Role of abscisic acid (ABA) and Arabidopsis thaliana ABA-insensitive loci in low water potential-induced ABA and proline accumulation. *J. Exp. Bot.* **57**, 201–212.
25. Ursache, R., Andersen, T.G., Marhavý, P., and Geldner, N. (2018). A protocol for combining fluorescent proteins with histological stains for diverse cell wall components. *Plant J.* **93**, 399–412.
26. Haseloff, J. (1999). GFP variants for multispectral imaging of living cells. *Methods Cell Biol.* **58**, 139–151.
27. R Development Core Team (2008). R: a language and environment for statistical computing (R Foundation for Statistical Computing).
28. Schindelin, J., Arganda-Carreras, I., Frise, E., Kaynig, V., Longair, M., Pietzsch, T., Preibisch, S., Rueden, C., Saalfeld, S., Schmid, B., et al. (2012). Fiji: an open-source platform for biological-image analysis. *Nat. Methods* **9**, 676–682.
29. Huber, W., Carey, V.J., Gentleman, R., Anders, S., Carlson, M., Carvalho, B.S., Bravo, H.C., Davis, S., Gatto, L., Girke, T., et al. (2015). Orchestrating high-throughput genomic analysis with Bioconductor. *Nat. Methods* **12**, 115–121.
30. Murashige, T., and Skoog, F. (1962). A revised medium for rapid growth and bioassays with tobacco tissue cultures. *Physiol. Plant.* **15**, 473–497.
31. Kondo, Y., Nurani, A.M., Saito, C., Ichihashi, Y., Saito, M., Yamazaki, K., Mitsuda, N., Ohme-Takagi, M., and Fukuda, H. (2016). Vascular cell induction culture system using Arabidopsis leaves (VISUAL) reveals the sequential differentiation of sieve element-like cells. *Plant Cell* **28**, 1250–1262.
32. Gutierrez, L., Mauriat, M., Guénin, S., Pelloux, J., Lefebvre, J.-F., Louvet, R., Rusterucci, C., Moritz, T., Guerineau, F., Bellini, C., and Van Wuytswinkel, O. (2008). The lack of a systematic validation of reference genes: a serious pitfall undervalued in reverse transcription-polymerase chain reaction (RT-PCR) analysis in plants. *Plant Biotechnol. J.* **6**, 609–618.
33. Czechowski, T., Stitt, M., Altmann, T., Udvardi, M.K., and Scheible, W.-R. (2005). Genome-wide identification and testing of superior reference genes for transcript normalization in Arabidopsis. *Plant Physiol.* **139**, 5–17.
34. Lovdal, T., and Lillo, C. (2009). Reference gene selection for quantitative real-time PCR normalization in tomato subjected to nitrogen, cold, and light stress. *Anal. Biochem.* **387**, 238–242.
35. Dekkers, B.J.W., Willems, L., Bassel, G.W., van Bolderen-Veldkamp, R.P., Ligtnerink, W., Hilhorst, H.W., and Bentsink, L. (2012). Identification of reference genes for RT-qPCR expression analysis in Arabidopsis and tomato seeds. *Plant Cell Physiol.* **53**, 28–37.
36. Love, M.I., Huber, W., and Anders, S. (2014). Moderated estimation of fold change and dispersion for RNA-seq data with DESeq2. *Genome Biol.* **15**, 550.

STAR★METHODS

KEY RESOURCES TABLE

REAGENT or RESOURCE	SOURCE	IDENTIFIER
Chemicals, peptides, and recombinant proteins		
Murashige and Skoog Medium (MS)	Duchefa Biochemie	Cat#M0222.0050
MES monohydrate	Duchefa Biochemie	Cat#M1503.0250
Bactoagar	Swab	Cat#B1000-1
Abscisic acid (ABA)	Sigma	Cat#14375-45-2
Polyethylene glycol 8000	Sigma	Cat#89510
Chloralhydrate	Sigma	Cat#15307
Urea	Sigma	Cat#57-13-6
Sodium deoxycholate	Sigma	Cat#1065040250
Xylitol	Sigma	Cat#X3375
Propidium iodide	Sigma	Cat#P4170
2,4-D	Sigma-Aldrich (Merck)	D70724-5G
Kinetin	Sigma-Aldrich (Merck)	K3378-1G
Critical commercial assays		
RNeasy Plant Mini Kit	QIAGEN	Cat#74904
iSCRIPT cDNA synthesis kit	Biorad	Cat#1708891
iQ SYBR Green Supermix	Biorad	Cat#17088882
Qubit BR RNA Assay	Invitrogen	Cat#Q10211
Deposited data		
Raw and processed RNaseq data files	This study	GEO: GSE169367
Experimental models: organisms/strains		
<i>Arabidopsis thaliana</i> : Col-0	Widely distributed	N/A
<i>Arabidopsis thaliana</i> : C24	Widely distributed	N/A
<i>Nicotiana benthamiana</i>	22	N/A
<i>Ptheirospermum japonicum</i>	23	N/A
<i>Solanum lycopersicum</i> cv. Moneymaker	Plantagen	N/A
<i>Solanum lycopersicum</i> cv. TinyTim	Plantagen	N/A
<i>Brassica napus</i> cv. Hanna	Lantmännen	N/A
<i>Brassica rapa</i> cv. Purple Top Milan	Impecta	N/A
<i>Arabidopsis thaliana</i> : <i>abi1-1C</i>	24	N/A
<i>Arabidopsis thaliana</i> : <i>SCR_{pro}:abi1-1</i> in Col-0 background	9	N/A
<i>Arabidopsis thaliana</i> : <i>UAS_{pro}:abi1-1</i> in Col-0 background	9	N/A
<i>Arabidopsis thaliana</i> : J0571 in C24 background	25	N/A
<i>Arabidopsis thaliana</i> : Q0990 in C24 background	25	N/A

(Continued on next page)

Continued		
REAGENT or RESOURCE	SOURCE	IDENTIFIER
<i>Arabidopsis thaliana</i> : J1721 in C24 background	25	N/A
<i>Arabidopsis thaliana</i> : <i>vnd1</i> in Col-0 background	26	N/A
<i>Arabidopsis thaliana</i> : <i>vnd2</i> in Col-0 background	26	N/A
<i>Arabidopsis thaliana</i> : <i>vnd3</i> in Col-0 background	26	N/A
<i>Arabidopsis thaliana</i> : <i>vnd6</i> in Col-0 background	26	N/A
<i>Arabidopsis thaliana</i> : <i>vnd7</i> in Col-0 background	26	N/A
<i>Arabidopsis thaliana</i> : <i>vnd1 vnd2</i> in Col-0 background	26	N/A
<i>Arabidopsis thaliana</i> : <i>vnd2 vnd3</i> in Col-0 background	26	N/A
<i>Arabidopsis thaliana</i> : <i>vnd1 vnd3</i> in Col-0 background	26	N/A
<i>Arabidopsis thaliana</i> : <i>vnd1 vnd2 vnd3</i> in Col-0 background	26	N/A
<i>Arabidopsis thaliana</i> : <i>vnd1 vnd2 vnd3 vnd7</i> in Col-0 background	This study	N/A
<i>Arabidopsis thaliana</i> : <i>VND1_{pro}:NLS-YFP</i> in Col-0 background	12	N/A
<i>Arabidopsis thaliana</i> : <i>VND2_{pro}:NLS-YFP</i> in Col-0 background	12	N/A
<i>Arabidopsis thaliana</i> : <i>VND3_{pro}:NLS-YFP</i> in Col-0 background	12	N/A
<i>Arabidopsis thaliana</i> : <i>VND5_{pro}:NLS-YFP</i> in Col-0 background	12	N/A
<i>Arabidopsis thaliana</i> : <i>VND7_{pro}:NLS-YFP</i> in Col-0 background	12	N/A
<i>Arabidopsis thaliana</i> : <i>6XABRE_A_{pro}:erGFP</i> in Col-0 background	8	N/A
<i>Arabidopsis thaliana</i> : <i>6XABRE_R_{pro}:erGFP</i> in Col-0 background	8	N/A
Oligonucleotides		
Oligonucleotides are specified in Table S2	This study	N/A
Software and algorithms		
Zeiss Zen Black 2.3 SP1	Zeiss	https://www.zeiss.com/
Zeiss Zen Blue 2.3 lite and 2.5	Zeiss	https://www.zeiss.com/
R 4.0.2 and R studio 1.2.5019	27	https://www.r-project.org/ ; https://rstudio.com/

(Continued on next page)

Continued

REAGENT or RESOURCE	SOURCE	IDENTIFIER
Microsoft Excel 2016	Microsoft	N/A
Illustrator 2020	Adobe	N/A
Affinity Designer 1.7	Affinity	N/A
Fiji/ImageJ 2.0.0 Win64 or 2.0.0-rc-68/1.52 h	²⁸	https://fiji.sc/
Bioconductor 3.11	²⁹	https://bioconductor.org/
Other		
Zeiss LSM780 confocal microscope	Zeiss	https://www.zeiss.com/
Zeiss LSM800 confocal microscope	Zeiss	https://www.zeiss.com/
Zeiss AxioScope A1	Zeiss	https://www.zeiss.com/
Leica M205 FA stereo-fluorescent microscope	Leica Microsystems	https://www.leica-microsystems.com/

RESOURCE AVAILABILITY

Lead contact

Further information and requests for resources and reagents should be directed to and will be fulfilled by the lead contact, Annelie Carlsbecker (annelie.carlsbecker@ebc.uu.se).

Materials Availability

There are no restrictions to the availability of newly generated resources in this study.

Data and code availability

The accession number for the transcriptome data reported in this paper is GEO: GSE169367.

EXPERIMENTAL MODEL AND SUBJECT DETAILS

Arabidopsis thaliana (L.) Heynh. Columbia-0 (Col-0), *Brassica napus* cv. Hanna, *Brassica rapa* cv. Purple Top Milan, *Nicotiana benthamiana*,²² *Pitheiospermum japonicum*²³ and *Solanum lycopersicum* cv. Moneymaker and Tiny Tim, were used in this study. All mutant and transgenic lines detailed in the [Key resources table](#) were in Col-0 background. All plant growth was carried out in growth rooms in long day conditions, 16 h light (22°C) and 8 h darkness (20°C) at light intensity of 110 μmol m⁻² s⁻¹.

METHOD DETAILS

Plant growth conditions

Seeds were surface sterilized using 70% Ethanol for 20 min and 95% Ethanol for 2–3 min, and then rinsed in sterile water four times. The seeds were imbibed and stratified for 48 h at 4°C, and plated on 0.5xMurashige and Skoog medium (MS)³⁰ supplemented with 1% Bactoagar and 0.05% MES monohydrate, pH 5.7–5.8. For all experiments, plants were grown vertically on 25 μm pore Sefar Nitex 03-25/19 mesh, and transferred to new plates by transferring the mesh with the plants on for minimal disturbance. For experiments involving transfer from ABA back to mock conditions, seedlings were instead transferred individually to prevent effects of residual ABA on the mesh. For ABA (Sigma) treatment, stock solutions of 50mM and 5mM ABA in 95% ethanol were used to make plates with ABA concentrations as indicated. Treatment with polyethylene glycol, was done with PEG 8000, as previously described.^{2,24} Briefly, 60ml of 550 g/l PEG solution in 0.5XMS was overlaid on plates containing 40ml of solid 0.5xMS media and left overnight. The excess PEG solution was discarded before transfer of plants to the plates.

For *Arabidopsis* phenotyping experiments, two-day old seedlings were transferred to 1 μM ABA containing plates for treatments of times indicated. For gene expression analysis, 4–5-day old seedlings were used. For phenotyping other species, seedlings were grown until roots reached approximately 1cm in length before transfer to ABA-containing plates.

All mutants or lines used in this study are listed in the [Key resources table](#). For generation of the *vnd1 vnd2 vnd3 vnd7* quadruple mutant, the *vnd1 vnd2 vnd3* triple mutant was crossed to the *vnd7* mutant, and segregating F2 seedlings were genotyped using the primers listed in [Table S2](#). The ABA responsive reporters used in this study are from Wu et al.⁸ and the VND transcriptional reporters are from Kubo et al.¹² For tissue specific expression of *abi1-1*, *UAS_{pro}:abi1-1*⁹ were crossed to Haseloff enhancer trap lines²⁶ and the resulting F1 seedlings were used for further analysis.

Phenotypic analysis

Xylem morphology quantification

For analysis of xylem morphology, roots were mounted directly in chloralhydrate solution, 8:2:1 chloralhydrate:glycerol:water (w/v/v), and visualized as described previously² using a Zeiss AxioScope A1 microscope at 40X magnification with differential interference contrast (DIC) optics. For quantification of phenotypes, the entire primary root or part of the root grown during the treatment times were analyzed for differences from wildtype pattern, separately for the distinct xylem axis positions (*px*, *omx* and *imx*). Phenotypes were categorized and the number of plants displaying a certain phenotype was used to calculate the frequency. Presence of more than one phenotype occurring in the same root was classified into a separate category.

Quantification of xylem differentiation

For determination of the point of xylem differentiation initiation, i.e., where SCW and lignification can be detected first relative the root tip, roots were cleared and stained with ClearSee solution containing calcofluor white and basic fuchsin.²⁵ Briefly, seedlings were fixed in 4% paraformaldehyde solution for 1 h at room temperature and washed with 1X PBS three times. The fixed tissue was incubated in ClearSee solution overnight and stained with calcofluor white and basic fuchsin. After staining, the tissue was washed in ClearSee and tile scans of roots from the root tip were acquired using Zeiss LSM780 inverted Axio Observer with supersensitive GaAsP detectors. Distances from the root tip to xylem vessel with bright fuchsin staining (lignin) at different positions in the xylem axis was measured by drawing a line from the root tip to the point of lignification using Zeiss Zen software.

Xylem differentiation at the inner metaxylem position

For early *imx* differentiation phenotypes, roots were mounted in chloralhydrate solution parallel to each other with root tips aligned on glass slides. A line was drawn on the glass slide at a distance of 7mm from the root tip and this 7mm section of the root from the root tip was analyzed for the presence of lignified metaxylem. Roots were scored for presence or absence of a lignified *imx* using Zeiss AxioScope A1 microscope. For *B. napus*, *B. rapa* and *S. lycopersicum*, roots were mounted similarly to *Arabidopsis* and the number of xylem vessels at 5mm from the root tip was quantified. For *P. japonicum* and *N. benthamiana*, xylem vessel number was quantified at 2mm from the root tip.

The number of primary roots analyzed in each experiment is represented in the individual figures. Most experiments were repeated at least three times with similar results.

Xylem trans-differentiation of cotyledon cells

For vascular induction in *Arabidopsis* cotyledons we followed the protocol used for xylem induction in cotyledons using bikinin with minor modifications.¹⁷ The modifications include the following: 1. In the induction medium, all components were like in Kondo et al.¹⁷ except that bikinin was replaced with 10 μ M ABA. 2. The time for induction was increased from 4 days to 6 days. At the end of the 6-day induction period, cotyledons were fixed like in Kondo et al.³¹ The samples were then washed with sterile water to remove traces of fixative solution. Samples were placed in a basic fuchsin-ClearSee mixture (final basic fuchsin concentration 0.1%–0.2% in ClearSee) overnight. The following day the samples were cleared with ClearSee and mounted on slides with ClearSee for visualization of autofluorescence (UV filter) or basic fuchsin staining (dsRED filter) with a Leica M205 FA stereofluorescent microscope. The area of ectopic lignification (autofluorescence) was calculated using ImageJ²⁸ and normalized to the total cotyledon area. Cotyledon veins were excluded from the quantification.

Confocal analysis

Roots were mounted in 40 μ M propidium iodide (PI) solution between two coverslips and imaged immediately. Confocal micrographs were captured using Zeiss LSM780 inverted Axio Observer with supersensitive GaAsP detectors. For calcofluor white 405nm laser was used for excitation and emission wavelengths 410–524nm were captured in the detector. For basic fuchsin images, 561nm excitation and 571–695nm emission. For reporter lines expressing GFP and stained with PI: 561nm excitation and 650–719nm emission for PI; 488nm excitation and 500–553nm emission for GFP. For reporter lines expressing YFP, 514nm excitation for both YFP and PI, 518–562 emission for YFP and 651–688nm emission for PI was used. For ectopic lignin assays: autofluorescence 405nm excitation and 410–518nm emission; basic fuchsin 561nm excitation and 595–710nm emission. For experiments involving quantification of fluorescence intensity all imaging parameters were kept the same when imaging mock and ABA-treated roots. The Zeiss Zen software was used to quantify YFP intensity. Region of Interests (ROI) encompassing nuclei in the *Arabidopsis* root meristem were used to measure average fluorescence intensity. Nuclei from similar regions in the root was used for mock and ABA treated samples.

Expression analysis by quantitative RT-PCR

RNA samples were extracted using the RNeasy Plant Mini Kit (QIAGEN), cDNA was synthesized using iScript reverse transcriptase enzyme. qRT-PCR analysis was performed as previously described using iQ SYBR Green Supermix in an iCycler iQ Real-Time PCR (Bio-Rad) instrument,² for primers see Table S2. The following program was used for the qRT-PCR analysis: initial denaturation 95°C for 3mins, 40 cycles of 95°C for 15sec, 60°C for 1min and was followed by melt curve analysis to confirm the absence of off target amplification. For *Arabidopsis*, either 1mm root tips or whole roots were used, as indicated in text. For *S. lycopersicum* (cv Tiny Tim), whole roots were collected after mock or 1 μ M ABA treatments for 6 h. Putative VND orthologs in tomato were annotated according to TAIR (<https://www.arabidopsis.org/>) and gene sequences obtained from Sol Genomics Network (<https://www.solgenomics.net/>). Primers used in this study are listed in Table S2. Three biological replicates were used for all samples and individual data points are represented in graphs. APT1 and GAPDH for *Arabidopsis*^{32,33} and ACTIN and TIP41 for tomato^{34,35} was used as reference genes, respectively.

RNAseq analysis

Five-day old *Arabidopsis* seedlings of Col-0, *vnd1 vnd2 vnd3* and *vnd7* were treated for 8 h with 1 μ M ABA or mock. Three biological replicates, each consisting of 50–100 seedlings, were collected for each treatment-genotype combination. The lower part of the root (1 cm) was collected directly in RLT buffer (QIAGEN) and frozen in liquid nitrogen. In an independent experiment, samples from *Arabidopsis* Col-0(*UAS_{pro}:abi1-1*)xC24, J1721>>abi1-1, J0571>>abi1-1 and Q0990>>abi1-1, mock and ABA treated, were similarly collected. RNA was extracted using the RNeasy Plant Mini Kit (QIAGEN). RNA concentration was measured with Qubit BR RNA Assay and quality and integrity of the RNA was checked with the Agilent Bioanalyzer 2100 system (Agilent Technologies, CA, USA). A total amount of 500ng RNA per sample was used for library preparation. Sequencing was performed by Novogene (UK) on their Illumina sequencing platform with paired-end read length of 150 and 250–300bp cDNA library resulting in 5.4 to 10.5 G raw data per sample. Initial processing of the reads as well as mapping was done by Novogene. Briefly, mapping to the *Arabidopsis thaliana* reference genome was done using Hisat2. Count files were generated using HTSeq. 96%–98% of the total reads were mapped to the *Arabidopsis* genome, whereby 94%–95% of the total reads were uniquely mapped.

Differential expression analysis was done independently for both experiments using DESeq2 in Bioconductor.^{29,36} For statistical analysis of ABA effects on the different genotypes compared to wildtype, a DESeq2 model including a combinatorial effect was used (~genotype+genotype:condition). Log₂fold changes were extracted from the pairwise comparison mock versus treatment for each genotype, while p values and adjusted p values were extracted from the comparison between the mutants/transactivation lines and wildtype. The effect of the different genotypes under mock condition was analyzed in an additional differential expression analysis and all values were extracted from the pairwise comparison of wildtype versus mutant. A cut-off > 0.5 was applied to the log₂FC of Col-0 mock versus ABA comparison as well as to the log₂FC of Col-0(*UAS_{pro}:abi1-1*)xC24 mock versus ABA. A list of xylem enriched genes from a single cell RNaseq¹⁰ was generated by subtracting genes from the endodermis, cortex, trichoblast, atrichoblast and QC-columella cluster from the xylem cluster and used to identify xylem expressed genes influenced by ABA.

QUANTIFICATION AND STATISTICAL ANALYSIS

For categorical data, Fisher's exact test using the `fisher.test` function in R²⁷ was performed for greater than 2x2 matrices (i.e., considering all phenotype categories in a sample) and p values less than 0.05 were considered significant. For other data, Two-way ANOVA, One-way ANOVA or Student's t test was used. Statistical tests and significance threshold used are mentioned in figure legends, and summary of the ANOVA statistics in figures is presented in [Data S2](#). The number of roots analyzed in all experiments are mentioned in the corresponding figures.